Available online at www.sciencedirect.com

ScienceDirect

Advances in Space Research xx (2021) xxx-xxx

ADVANCES IN SPACE RESEARCH
(a COSPAR publication)

www.elsevier.com/locate/asr

Solar jets observed with the Interface Region Imaging Spectrograph (IRIS)

Brigitte Schmieder[a,b,c,*], Reetika Joshi[d], Ramesh Chandra[d]

[a]LESIA, Observatoire de Paris, Université PSL, CNRS, Sorbonne Université, Université de Paris, 5 place Jules Janssen, 92190 Meudon, France
[b]Centre for Mathematical Plasma Astrophysics, Dept. of Mathematics, KU Leuven, 3001 Leuven, Belgium
[c]University of Glasgow, Glasgow, Scotland
[d]Department of Physics, DSB Campus, Kumaun University, Nainital – 263 001, India

Abstract

Solar jets are impulsive, collimated plasma ejections that are triggered by magnetic reconnection. They are observed for many decades in various temperatures and wavelengths, therefore their kinematic characteristics, such as velocity and recurrence, have been extensively studied. Nevertheless, the high spatial resolution of the Interface Region Imaging Spectrograph (IRIS) launched in 2013 allowed us to make a step forward in the understanding of the relationship between surges and hot jets. In this paper we report on several results of recent studies of jets observed by IRIS. Cool and hot plasma have been detected with ejections of cool blobs having a speed reaching 300 km s^{-1} during the impulsive phase of jet formation and slow velocity surges surrounding hot jets after the reconnection phase. Plasma characteristics of solar jets, such as the emission measure, temperature, and density have been quantified. A multi-layer atmosphere at the reconnection site based on observed IRIS spectra has been proposed. IRIS evidenced bidirectional flows at reconnection sites, and tilt along the spectra which were interpreted as the signature of twist in jets. The search of possible sites for reconnection could be achieved by the analysis of magnetic topology. Combining Solar Dynamics Observatory/Helioseismic Magnetic Imager (SDO/HMI) vector magnetograms and IRIS observations, it was found that reconnection site could be located at null points in the corona as well as in bald patch regions low in the photosphere. In one case study a magnetic sketch could explain the initiation of a jet starting in a bald patch transformed to a current sheet in a dynamical way, and the transfer of twist from a flux rope to the jet during the magnetic reconnection process.

Keywords: Solar jets; Solar flares; Magnetic field

1. Introduction

Jets are plasma ejections along collimated magnetic field lines. They act as a source for transporting mass and energy and can contribute to the heating of the solar corona and the acceleration of the solar wind. They are the key tool to probe the broad dimensions of the heliospheric problems. Many authors have analysed these small-scale solar ejections, from Hα surges (Roy, 1973; Schmieder et al., 1983; Uddin et al., 2012) to X-ray jets (Shibata et al., 1992) or X-ray coronal loops (Schmieder et al., 1995). All the literature concerning jets from a theoretical point of view as well from observations is summarized in recent reviews (Raouafi et al., 2016; Pariat et al., 2016; Shen, 2021; De Pontieu et al., 2021).

Several recent studies focused on recurrent homologous jets observed in different wavelengths such as in Hα (Asai et al., 2001; Chandra et al., 2017), in EUV (Chae et al., 1999; Jiang et al., 2007; Schmieder et al., 2013; Chandra et al., 2015; Joshi et al., 2017), and in X-rays (Kim et al., 2001; Kamio et al., 2007; Sterling et al., 2016). The characteristics of jets are very well described from jet observations made by the Atmospheric Imaging Assembly (AIA, Lemen et al. (2012)) telescope on board the Solar Dynamics Observatory (SDO, Pesnell et al. (2012)) satellite (Kayshap & Dwivedi, 2017; Joshi et al., 2017). The range of jet velocities is between 100 to 300 km s^{-1} and the

*Corresponding author
Email addresses: Brigitte.Schmieder@obspm.fr (Brigitte Schmieder), reetikajoshi.ntl@gmail.com (Reetika Joshi), rchandra.ntl@gmail.com (Ramesh Chandra)

https://dx.doi.org/10.1016/j.jasr.xxxx.xx.xxx
0273-1177/

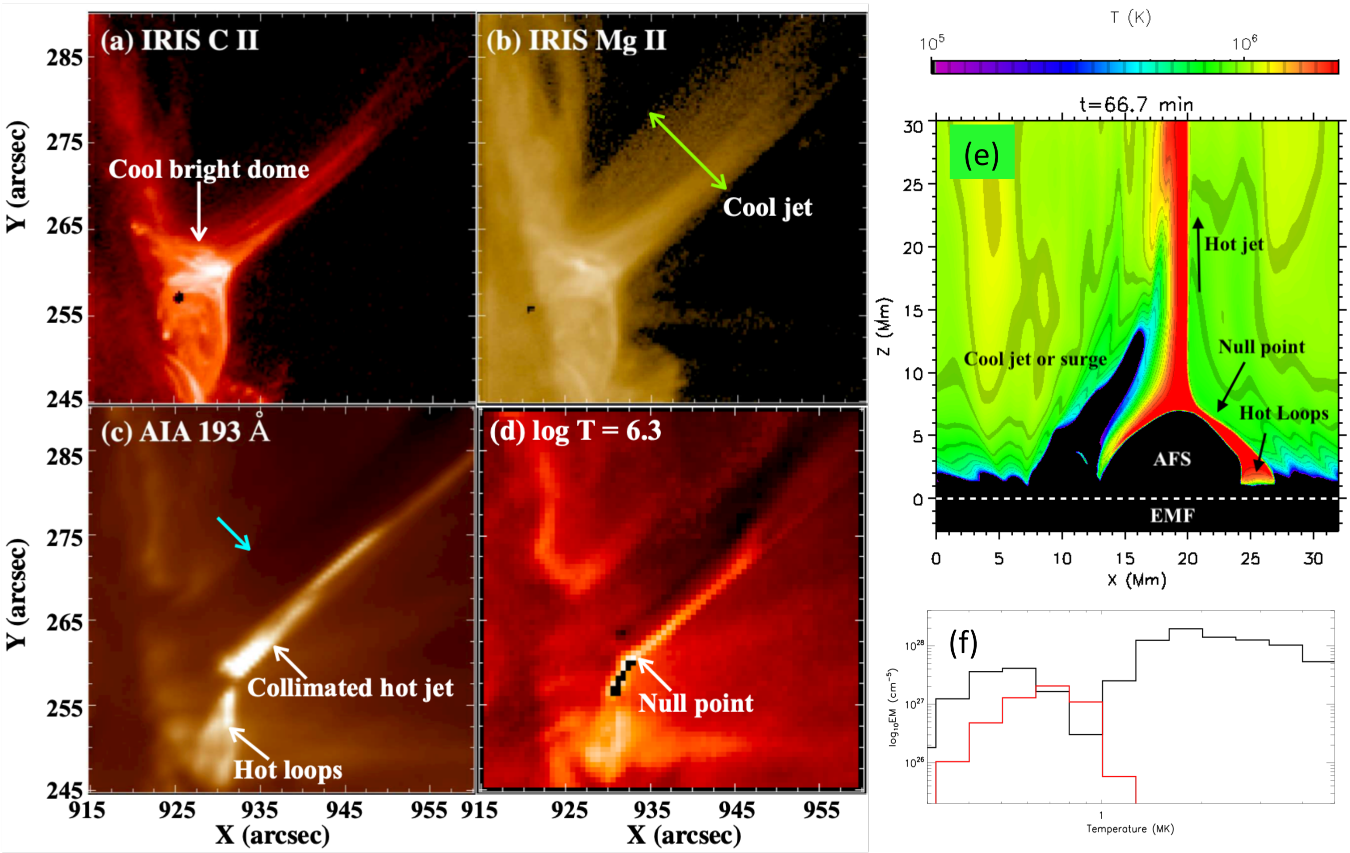

Fig. 1. IRIS slit jaw images of a jet on April 4 2017 observed in cool plasma (CII and MgII) (top panels a-b) and in hot plasma in AIA 193 Å image and temperature map for log T (K) = 6.3 (panels c-d). Panel (e): numerical simulation of a cool surge surrounding a hot jet during reconnection fitting well with the jet observations. Panel (f): emission measure (EM) in the jet (red) and its base (black) (adapted from Nóbrega-Siverio et al. (2017); Joshi et al. (2020a)).

length can be as short as 5 Mm and as long as 100 Mm. Trigger mechanisms of jets are based on magnetic reconnection depending on the magnetic configuration of the region with flux emergence and cancellation (Archontis & Hood, 2009; Török et al., 2009; Moreno-Insertis & Galsgaard, 2013; Priest et al., 2018) or with rotation of sunspot (Pariat et al., 2009; Curdt et al., 2012). Jets occur at different locations, in the center or at the border of active region (Chandra et al., 2017; Joshi et al., 2017), at the edge of coronal holes (Moreno-Insertis et al., 2008; Moreno-Insertis & Galsgaard, 2013) or at light-bridges (Robustini et al., 2016; Yang et al., 2020; Bharti et al., 2020). Spicules are also considered as chromospheric jets and well studied with recent instrumentation (De Pontieu et al., 2021). A new kind of jet/spicule has been discovered with IRIS related to the activity of filaments and prominences. Photospheric motions are favouring the braiding of magnetic field lines which could interact between them and produce nano jets through reconnection in loops and prominences (Chen et al., 2017; Huang et al., 2018; Chitta et al., 2019; Chen et al., 2020; Antolin et al., 2021). The motivation of this paper is based on new imaging and spectral observations obtained with IRIS which covers a large chromospheric and transition region temperature range. Therefore they are very complementary to the high spatial and temporal imaging observations of SDO/AIA instrument. We present a few studies of jets observed with IRIS in a broader context (Joshi et al., 2017, 2020a,b, 2021b,a). These observations allow us to answer several questions. What are the plasma characteristics of jets (temperature, density)? Section 3.1 is focused on hot and cool plasma properties. Spectral diagnostics with OIV lines allow to retrieve accurate density values for different types of jets. The spire jet density is one or two orders of magnitude less than the jet base density. What is the dynamic of jets in 3D? Section 3.2 presents the explosive dynamic nature of jets, their morphology with examples of bilateral flows, rotation and twist measured in IRIS spectra. Why is there cool material over hot material in the flare site? From where the twist comes in the jets? proposed during magnetic reconnection at the jet base from a flux rope to a jet with plasmoid ejections is presented (Sections 4.1 and 4.2). We discuss on a multi thermal flare model deduced from the IRIS spectra. Electric currents measured at the jet base suggest the formation of quasi-separatrix layers (Section 4.3). Finally we discuss on the benefits from the observations of IRIS in relatively cool temperature jets for braiding loops and nano jets (Section 4.4).

2. Observations

IRIS (De Pontieu et al., 2014) observed many jets since its launch in 2013 in different modes of observations, from very

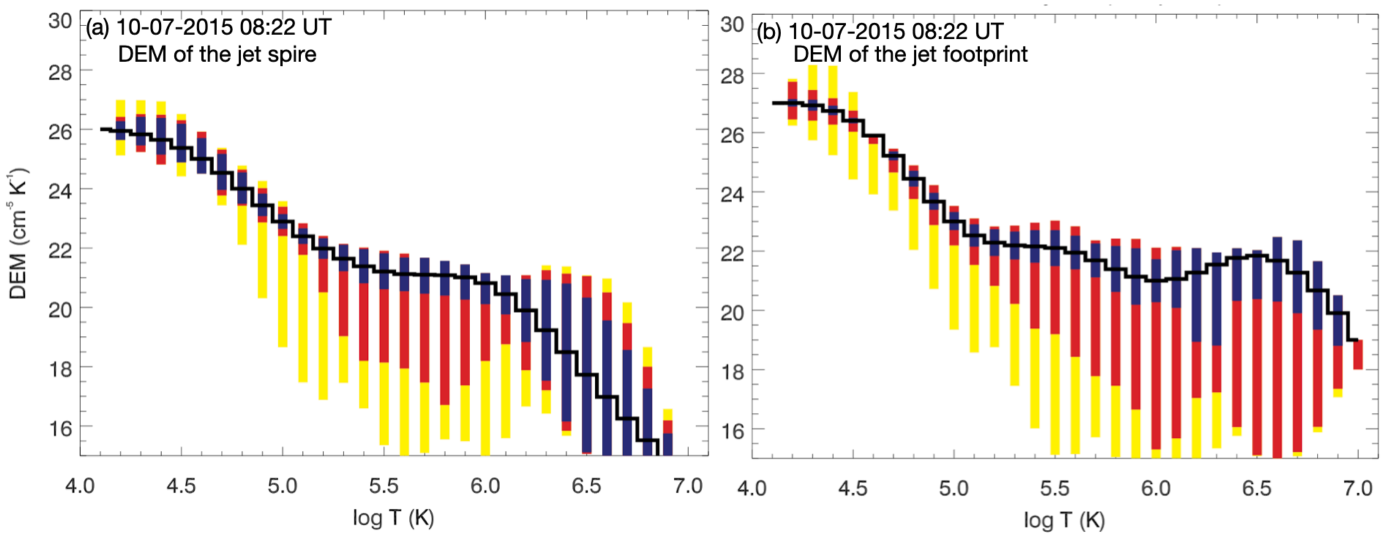

Fig. 2. Differential emission measure (DEM) obtained by combining cool lines of IRIS and AIA filter data of July 10 2015. The estimates of uncertainties on the best-fit DEM curves are obtained by randomly varying the input intensities by 20% after performing 300 Monte Carlo (MC) simulations on the intensities. In each temperature bin, the errors are plotted with different colour bars. 50% of solutions closest to best-fit DEM are shown by blue, 80% by red and 95% by yellow. (adapted from Mulay et al. (2017a).

dense, medium or coarse rasters and, simultaneously with slit jaw images (SJI) having the same coordinate center with a maximum field of view of 167 arcsec × 175 arcsec. Usually IRIS observes in four channels around 1330 Å, 1400 Å, 2796 Å, 2832 Å including CII, SiIV, MgII lines, and the UV continuum, respectively. CII lines are formed around T = 30000 K and SiIV lines around 80000 K, while MgII lines are formed at chromospheric temperatures between 8000 K and 20000 K. The cadence of SJIs is a few seconds to one minute and the pixel resolution size is 0.35 arcsec. The field of view of the rasters can be reduced to one slit (sit and stare mode) or 4 slits (field of view 16 arcsec × 60 arcsec) or 32 slits (FOV = 62 × 60 arcsec). From the rasters Dopplershift line width can be directly retrieved for each pixel after fitting the profiles with Gaussian function routine available in Solarsoft. IRIS brings to us an important knowledge about chromospheric and transition region plasma and complement AIA images which allow to compute with accuracy the transverse velocity of jets.

3. Solar jets observed with IRIS

3.1. Plasma characteristics of hot and cool jets

IRIS with its spectral mode allowed us to get quantitative results on the emission measure (EM), temperature and electron density.

Working on six recurrent jets in the active region NOAA 12644 on April 4, 2017, cool IRIS surges as well as hot AIA filter jets were detected by Joshi et al. (2020a) (Fig. 1). A fine co-alignment of the AIA and IRIS data shows that the hot jets are collimated and observed in the hot temperature filters. They have high velocities, around 250 km s^{-1} and are accompanied by cool surges surrounding the hot jets and ejected kernels that both move at about 45 km s^{-1}. The jets were initiated at a null point at the top of a canopy-like double-chambered structure with cool emission on one side and hot emission on the other side as proposed in the emerging flux simulations of Nóbrega-Siverio et al. (2017). Joshi et al. (2020a) used the AIA filters to study the temperature and the EM of the jets using the filter ratio method (Fig. 1 panel (f)). The EM (cm^{-5}) reaches 10^{28} for coronal temperature in the jet base and 10^{27} in the jet spire for this case.

Cool and hot emission in other recurring active region jets with significant cool emission at foopoints and along the jets are frequently observed with IRIS (Mulay et al., 2016, 2017b,a; Kayshap et al., 2021; Nóbrega Siverio et al., 2021). The DEM analysis in Mulay et al. (2017a) took into account the IRIS data with the EUV AIA data of the cool and hot emission in the spire and the footpoint regions (Fig. 2). The emission was peaked at log T (K) = 5.6–5.9 which is a transition zone temperature and 6.5 which is coronal emission, respectively. The differential emission measure (DEM) curves show the presence of hot plasma (T = 3 MK) in the footpoint region. They confirmed this result by estimating the Fe XVIII emission from the AIA 94 Å channel which was formed at an effective temperature of log T (K) = 6.5. The average EM (cm^{-5}) was increasing by three orders of magnitude reaching 10^{31} for the spire and 10^{32} for the jet base compared with results using only AIA data (Mulay et al., 2017b; Mulay, 2018; Joshi et al., 2020a; Kayshap et al., 2021).

In the IRIS spectra OIV lines are observed in the SiIV waveband at the location of jets (Fig. 3). OIV lines observed in the IRIS FUV spectra allow to perform density diagnostics on the jet material at transition region temperatures. The ratio of OIV intensities allow to compute the electron densities in case of SiIV is not too optically thick (Judge, 2015). Cheung et al. (2015) used two different line ratios to measure the densities. The first is the ratio of the OIV 1401.16 and 1404.82 lines in

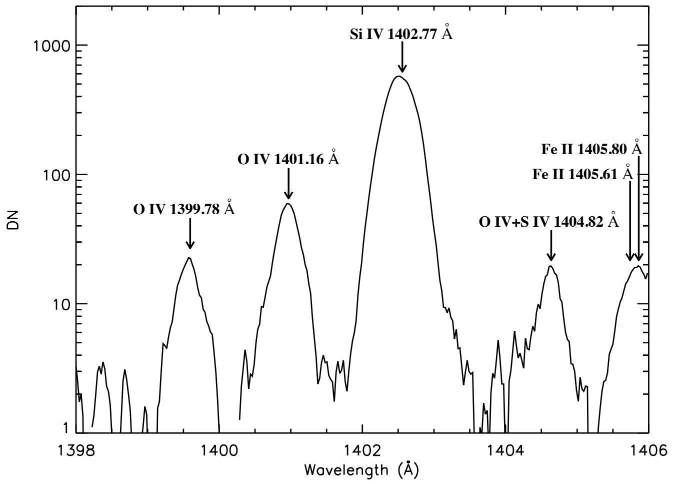

Fig. 3. IRIS spectra (in log DN units) for the footpoint region of jet obtained for the SiIV 1403 Å window on March 22 2019 (Joshi et al., 2021a). At the time of the reconnection OIV lines are detectable in the mini flare.

jets. The 1404.82 line is blended with a SIV line, so they used the SIV 1406.02 line assuming an optically thin emission to extract the intensity of OIV 1404.8. The OIV 1404.8 line is not always present in the spectral readout window of IRIS. However, in a number of slit positions where there is sufficient blueshift, they found the ratio OIV 1401.1/1404.8 to be in the range 4.0-4.5. For a temperature range of log T (K) = 4.5-5.5 (derived from the ratio of SIV 1404.8 to SIV 1406.02), this ratio gives densities ranging from log Ne (cm^{-3}) = 10.8-11.0. Similarly, a ratio computed for the 1399.77 and 1401.16 lines of OIV has values in the range 0.29-0.35, which yields electron densities of log Ne (cm^{-3}) = 10.8-11.2.

Using the same diagnostics rather low values for temperature (log T (K) = 5.42) and density (log Ne (cm^{-3}) = 10.3) were derived for short corona mini-jet in clusters above activated prominence fine structures (Chen et al., 2020).

Cai et al. (2019) found the temperature of the plasma in the jet heated to atleast T= $10^{5.6}$ K. The electron density is about log Ne (cm^{-3}) = 11 according to the intensity ratios of the OIV 1399.77/1401.16 doublet and SiIV 1402.77/OIV 1401.16 lines. Mulay et al. (2017a) found in their analysis electron densities (cm^{-3}) around 10.3 in the spire and 10.9 in the footpoint while Joshi et al. (2021a) found in the jet canopy roughly log Ne (cm^{-3}) = 11 ± 0.3. At the base of jet where the reconnection occurred the shape of the profiles did not allow them to distinguish if there were many components or if it was due to microturbulence, therefore the electron density diagnostics was difficult to be applied (Joshi et al., 2021a).

The study by Nóbrega Siverio et al. (2021) concerns OIV emitting layers around cool surges (T=6000 K) observed in MgII line profiles. With the OIV ratio diagnostics they found electron density (cm^{-3}) values of the order of 1.6×10^{11} to 10^{12}. This result was confirmed by numerical experiments performed with the Bifrost code. Those higher values for jets correspond to those obtained for Hα surge (Schmieder et al., 1988, 1995) and for transition regions like in plage and bright point (Polito et al., 2016).

3.2. Bidirectional flows, rotation and twist in IRIS spectra

Rotational motion is an important property of the jet-like structures in the solar atmosphere. On the basis of Doppler velocity, it is frequently reported that typical coronal/chromospheric jets reveal blue-shifts at one edge and red-shifts at the other. It is well observed in Hα (Ruan et al., 2019) as well in hotter lines (Pike & Mason, 1998) observed with the Coronal Diagnostic Spectrometer (CDS, Harrison et al., 1995) and the Solar Ultraviolet Measurements of Emitted Radiation (SUMER, Wilhelm et al., 1995; Curdt & Tian, 2011) instrument. Both studies used the same OIV transition region line, which forms at log T (K) = 5.4 and they concluded that the spatial pattern of Dopplershifts blue on one side and red on the other side was an evidence for helical motion. Similar interpretation is taken for IRIS Doppler maps by different authors (Cheung et al., 2015; Ruan et al., 2019; Kayshap et al., 2021).

In Ruan et al. (2019) a jet occurred due to reconnection of field lines pushed upwards by an emerging flux (Fig. 4). The reconnection point is in the corona (shown as point B) and bidirectional flows of the order of ±200 km s^{-1} are observed in the spectra crossing the site, mainly in CII and SiIV (bottom panels). The jet crossed by the IRIS slit shows a blue and red shift pattern. Simultaneous observations in Hα show the same blue/redshift pattern. Such patterns suggest helical motion along the jet axis. While Moreno-Insertis & Galsgaard (2013) mention that the erupting flux ropes in the simulation seem to rotate as if they were converting twist into writhe, the possible helical motions of the jets themselves were not explicitly studied. The conclusion of Cheung et al. (2015) concerning the IRIS Doppler shift maps was that they share considerable resemblance to synthetic Doppler maps of Fang et al. (2014), who carried out MHD simulations of jets resulting from the interaction of a twisting flux tube emerging from the solar convection zone into a coronal layer with ambient inclined field.

In the jet study of Joshi et al. (2020b), the IRIS slit was crossing the jet base and a part of the jet (Fig. 5 panel a). At the pixel of the reconnection site, the Mg II line profile is the most extended one on the blue and red sides like in bidirectional outflows similar to the observations of Ruan et al. (2019) and Cai et al. (2019). The reconnection site MgII profile is identified at pixel y=75 in Fig. 5 panel (e)). Using a cloud model method they could interpret this wide profile by the presence of cool clouds ejected with a velocity of -300 km s^{-1}. Simultaneous SiIV profiles exhibit similar behaviour with large blueshifts. Over these wide profiles NiII and FeII narrow lines were detected in absorption similarly as in IRIS bomb profiles (Peter et al., 2014; Grubecka et al., 2016). Therefore with all the information in the sample of IRIS spectra combined with AIA multi wavelength filtergrams they could propose a synthesized empirical flare model (see Fig. 6 right panel) (Joshi et al., 2021b,a).

In Fig. 5 panel (b) in the northern and southern parts of the reconnection site, the authors note that the spectra shows a tilt. The MgII profiles are not symmetrical all along the slits. Therefore, with the existence of this gradient the tilt is obvious. The tilt is characterised by the gradient of the Dopplershifts that exist for profiles along the jet cross section at a given time. The line profiles of MgIIk line show important extensions of

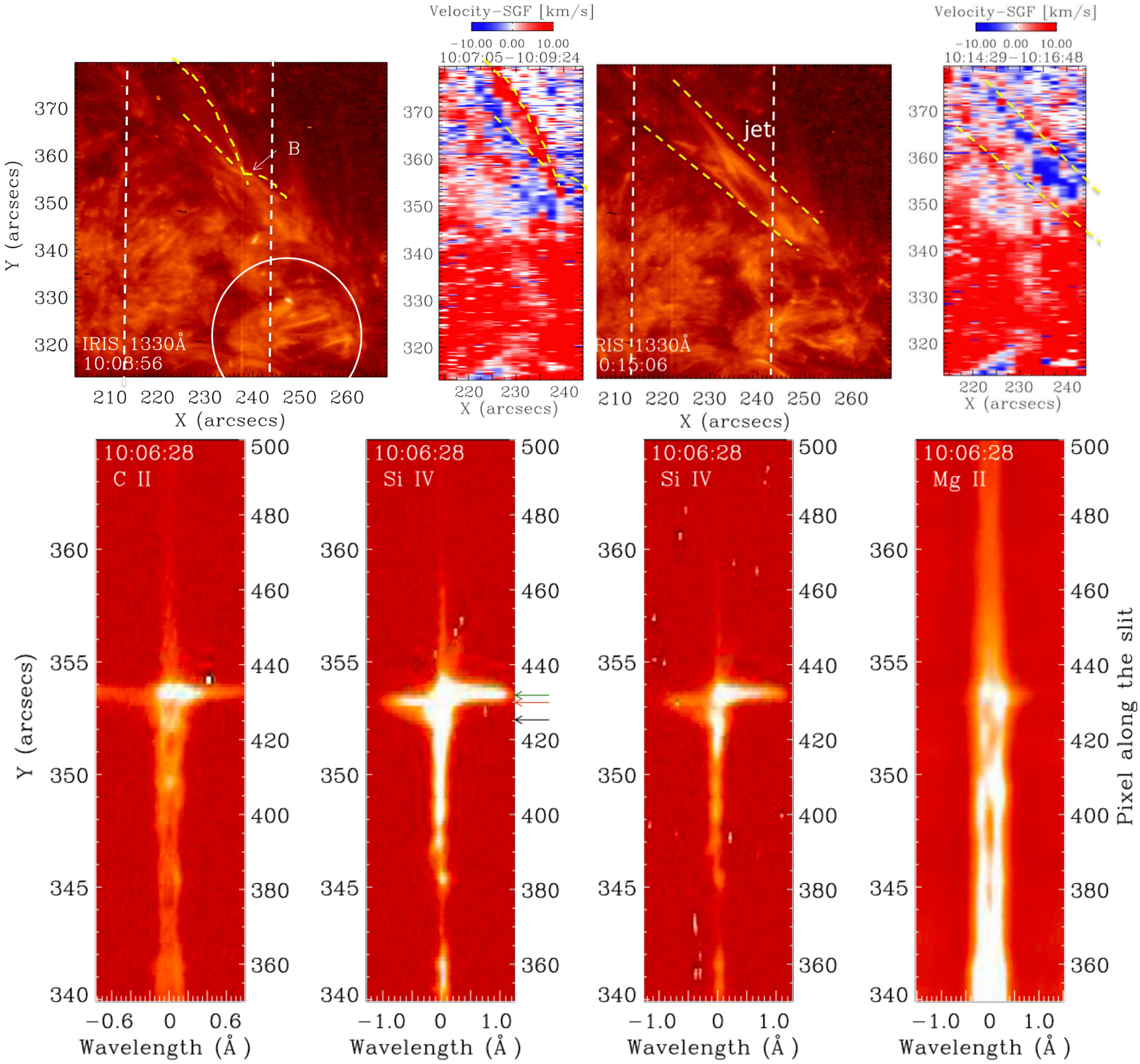

Fig. 4. Jet observed with IRIS SJI and Doppler maps with blue and redshifts showing a rotation around its main axis observed on March 30 2017 (top panels) and bidirectional flows at the reconnection point in B in several lines (bottom panels). The circle in the top left panel indicate the location of the emerging flux visible with arch filament system above. The vertical lines indicate the field of view of the rasters and the Doppler maps. The bottom panel shows the spectra of CII, SiIV (1393.8 and 1402.8 Å), and MgII. The spectra of CII, SiIV and MgII lines are vertical and CII and Si IV spectra (but not cool lines of MgII) show an horizontal bright feature indicating high blue and redshifts around 200 km s^{-1} (adapted from Ruan et al. (2019)).

the wings at 02:05:39 UT (Fig.5 panels c-h) . The Dopplershift velocity of the cool material along the west side has values of between 30 km s^{-1} to 100 km s^{-1} and on the east side between -300 km s^{-1} to -30 km s^{-1}. This means that one part of the cool material is red-shifted while the other part is blue-shifted i.e. coming towards us. A similar behaviour is observed in the four positions of the slit for MgII, CII, and SiIV lines. The tilt in the four SiIV spectra is even more readily visible because SiIV is a transition region line with only one emission peak when compared to chromospheric lines with two peaks.

The tilt in the spectra finally reach an extension around 15 Mm, which represent the size of the cross section of the jet. The authors interpret this tilt by the rotation of a structure at the base of the jet or possibly cool plasma that follows helical structures. Tilt of spectra along a slit crossing the section of the jet was first observed for prominences (Rompolt, 1975) and interpreted as rotating prominences before eruption.

3.3. *Light bridge jets*

With the high spatial and temporal resolution SJIs from IRIS at 1330 Å, Bharti (2015) were able to demonstrate fine scale details of jets above a light bridge (LB) in the transition zone temperature. Low altitude reconnection has been suggested as the mechanism to produce such an activity (Bharti et al., 2007). Shimizu (2011) reported about intermittent plasma ejections above a LB for a few days, accompanied with a change in the

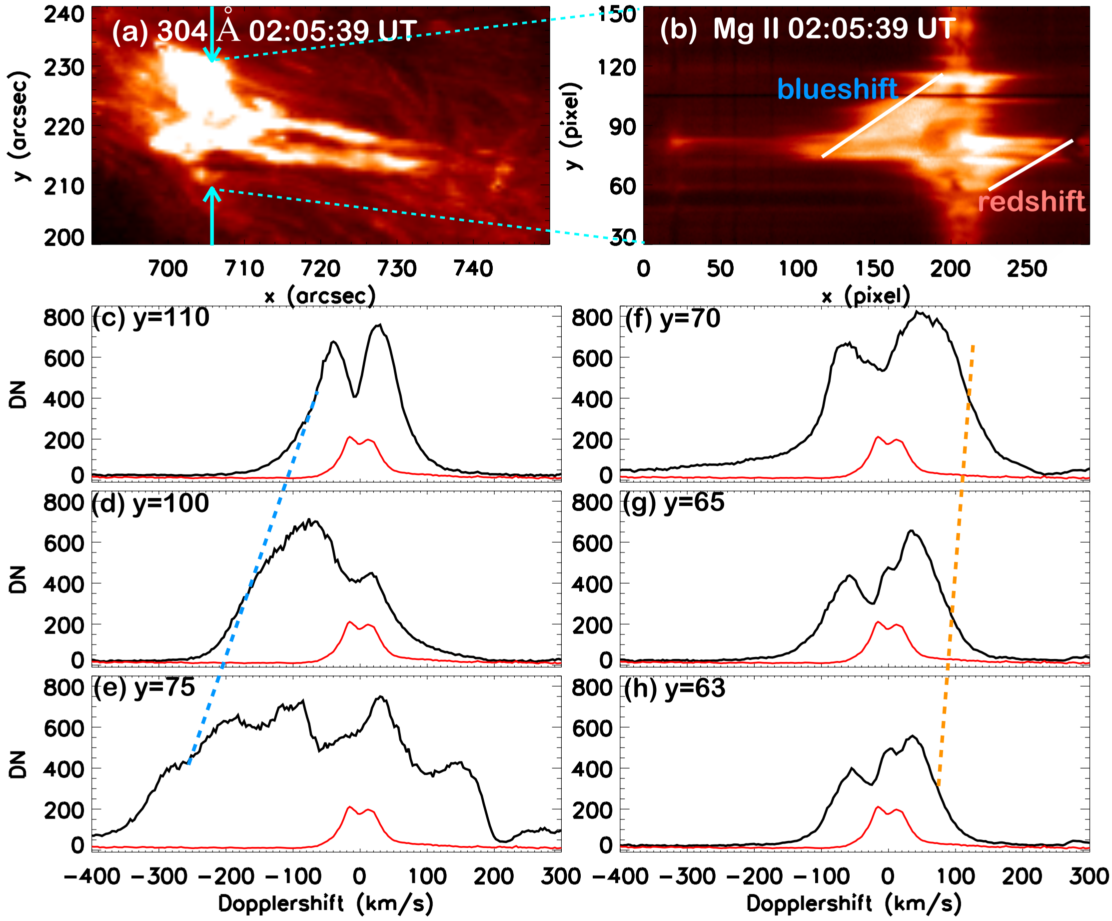

Fig. 5. Bright jet with two branches inserting a cool dense surge in AIA 304 Å observed on March 22 2019 (panel a). The cyan arrows show the location of the slit position 1. The MgII line spectra is crossing the reconnection site (panel b). Red and blue shift wings are shown by the white tilted lines on the left (blueshift) and right (redshift) in the spectra. The bottom rows (c-h) show the MgIIk line profiles for different y values using unit of velocity in the x axis. Panels c-e concern the blue shift profiles shown by the tilted blue dashed line corresponding to strong blueshifts (-300 to -100 km s^{-1}). Panels f-h show the red shift profiles. Redshifts (80 to 100 km s^{-1}) are shown by the red dashed tilted line. The red and blue dashed lines are passing through the inflexion points of the line profiles in panels c-h). Red profiles are reference profile in each panel c to h (adapted from Joshi et al. (2020b)

photospheric magnetic flux density and inclination. Shimizu et al. (2009) proposed a model where the LB is considered as a highly twisted current-carrying flux tube lying below the background field that forms a cusp-like shape above the LB. The proposed geometry then produces opposite polarity field at one side of LB and led to reconnection. According to Toriumi et al. (2015), the presence of patches of high vertical current of opposite sign is indicative of magnetic shear which is a favorable condition for magnetic reconnection. However jets in penumbra sunspots with LB are initiated by magneto convective process (Bharti et al., 2020). According to the former authors current layers are formed at the edges of the convective fine structure, due to the shear between their horizontal field and the ambient vertical field. The reconnection could be caused by an opposite polarity field produced by the bending of field lines by convective downflows at the edge of pore fine structure. Surges have been detected at the edge of LB in vortex formations due to the high shear existing at the edge of LB (Yang et al., 2020). IRIS spectra would be interesting to see the Dopplershifts in these reconnection sites.

4. Magnetic configuration in the jet environment

4.1. Shear between emerging flux: Transfer of twist

The jet with a strong tilt in the spectra studied in Joshi et al. (2020b) is originated in a region where two emerging magnetic fluxes (EMFs) collapsed (Fig. 6 left panel). Magnetic vector maps exhibit a long sigmoidal flux rope (FR) along the polarity inversion line between the two EMFs, which is the site of the reconnection. Before the jet, an extension of the FR was present and a part of it was detached and formed a small bipole with a bald patch (BP) region, which dynamically became an X-current sheet over the dome of the eastern EMF where the reconnection took place. This view is consistent with simulations of IRIS bombs proposed by Hansteen et al. (2019).

At the time of the reconnection, the MgII spectra exhibited a strong tilt, this was the signature of the transfer of the twist to the jet (Fig. 5). A comparison of the vector magnetic and electric current maps with numerical magnetohydrodynamics (MHD) simulations (Janvier et al., 2013; Aulanier et al., 2012; Aulanier & Dudík, 2019) confirms the existence of the long FR. The authors conjectured that there was a transfer of twist to

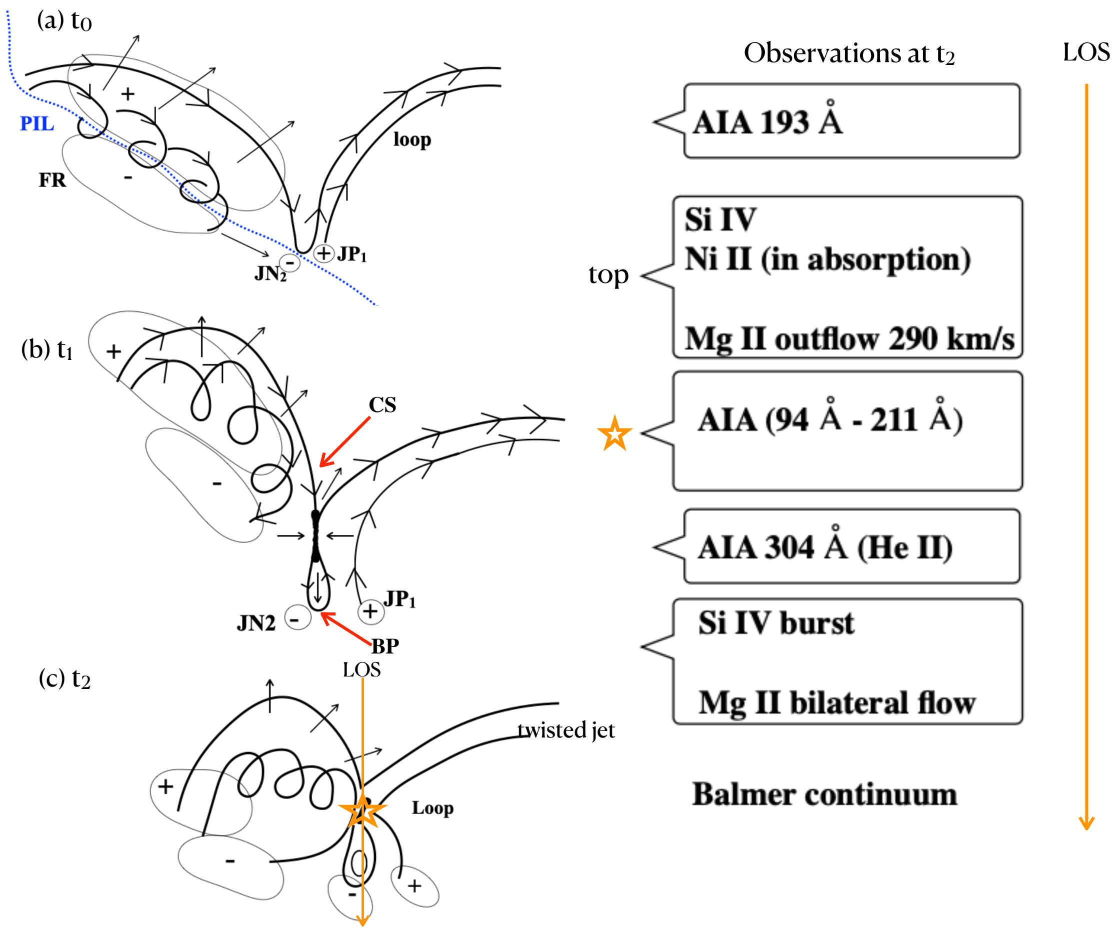

Fig. 6. Sketch of transfer of twist from a flux rope (FR) to a jet during reconnection in a bald patch (BP) transformed dynamically to a X-point current sheet; (*left panels*): at t_0 (panel a) two loop systems are approaching at the bipole JP1 and JN1, at t_1 (panel b) they are tangent at the BP forming a current sheet (CS) and at t_2 (panel c) there is the reconnection in the CS (orange star); (*right panel*): flare atmosphere model along the line of sight (LOS) during t_2. The sketch and the flare model are deduced from the observations of IRIS, AIA and HMI vector magnetograms on March 22 2019 (adapted from Joshi et al. (2020b)

.

the jet during the extension of the FR to the reconnection site without FR eruption. The reconnection would start in the low atmosphere in the BP reconnection region and extend at an X-point along the current sheet formed above like in the 3D MHD simulations of Hansteen et al. (2019) and Wyper et al. (2019).

For this event, Joshi et al. (2020b) could propose a multi thermal atmosphere model of the mini flare at the jet base as it was mentioned in the previous section (Fig. 6 right panel). The reconnection was accompanied by a bombardment of energetic electrons detected by hard X-ray emission measured by the FERMI/Gamma Burst Monitor (GBM, Meegan et al., 2009) (Joshi et al., 2021b). These energetic particles produced an enhancement of the Balmer continuum observed by IRIS. The good timing was the main favorable argument of this relationship. This phenomena is commonly observed for GOES X-class flare (Heinzel & Kleint, 2014; Kleint et al., 2016, 2017). Therefore Joshi et al. (2021b) concluded that the energetic electrons could be efficient for a B class flare only if reconnection occurred in a tiny area smaller than the IRIS spatial resolution.

4.2. Emerging flux models

In Joshi et al. (2020a) the series of jets and surges provides a good case study for testing the 2D and 3D magnetohydrodynamic emerging flux models even the jets were observed at the limb (Nóbrega-Siverio et al., 2017) (Fig. 1 panel e). The double-chambered structure that is found in the observations corresponds to the regions with cold and hot loops that are in the models below the current sheet that contains the reconnection site. The cool surge with kernels is comparable with the cool ejection and plasmoids that naturally appears in current sheet models (Ni et al., 2016, 2021).

4.3. Current sheet formation initiating jets

Accumulation of electric currents observed in photospheric magnetic vector maps is a good indicator for predicting flares, eruption and jets. Photospheric motions of magnetic polarities lead to stressed magnetic field lines which can release energy during reconnection. Photospheric electric current pattern evolution was observed of the jet bases (Guo et al., 2013). The authors found in the photospheric magnetic topology analysis that the pattern was associated with quasi-separatrix layers (QSL) deduced from magnetic extrapolation. There was a strong correlation between the built up of electric currents along the QSLs and the flux evolution of the jet base.

The built up of electric current is directly tied to photospheric motions. An other case on March 22, 2019 where IRIS jets were strongly related to photospheric motions which built up strong electric currents detected in HMI vector magnetic field maps (Joshi et al., 2020b). In that paper it was also suggested that electric currents were storage in the remnant FR magnetic field lines overlying the emerging dome. The transfer of twist occurred between the FR and the jet during reconnection.

4.4. Braiding loops and nano jets

Bidirectional flows were detected during the reconnection in the IRIS spectra as Dopplershifts (Ruan et al., 2019; Joshi et al., 2020b). Therefore the direction of bidirectional ejections could be perpendicular to the apparent transverse flows of the jets if measured in the sky plane. The bidirectional flows come from the reconnection-jet at the reconnection site (a few pixels in IRIS spectra). This phenomena is similar to the nano jets observed during the braiding of magnetic field lines of a loop attached to a filament (Antolin et al., 2021). The change of curvature of the field lines leads to the release of electric currents stored in the field lines and nano jets were detected in the IRIS spectra of transition zone plasma with speed of 200 km s^{-1}. Recently a statistical analysis of 43 nano jets observed with IRIS was done by Chen et al. (2020) where the jets were explained by fine-scale external/internal magnetic reconnection. Antolin et al. (2021) used MHD simulations to demonstrate that nano jets could be a consequence of the slingshot effect from the magnetically tensed, curved magnetic field lines reconnecting at small angles and produced coronal heating plasma at the reconnection site. Such release of energy could relatively be frequent in the corona as predicted by Parker (1988) and Demoulin & Priest (1997) and observed recently with Solar Orbiter, named as campfires (Berghmans et al., 2021). Dissipation of magnetic energy in the corona requires the creation of very fine scale-lengths because of the high magnetic Reynolds number of the plasma. The formation of current sheets is a natural possible solution to the heating problem and it is known that magnetic field stressed by continuous photospheric motions through a series of equilibria can easily form such sheets (Demoulin & Priest, 1997).

5. Summary and Conclusion

Recent jet observations with IRIS, spectra and SJIs, benefit from the high spatial resolution of the instrument (pixel size = 0.167 arcsec) and the high temporal cadence, never reached for chromosphere and transition region temperature spectra. These observations revealed that solar jets are very dynamic and have an impulsive nature like explosive events. Jet base is heated over a large range of temperatures. The reconnection can be accompanied by energetic electron ejections like in X-ray flares. Bidirectional flows are detected in reconnection sites, they correspond to jet-reconnections (Ruan et al., 2019; Joshi et al., 2021a; Antolin et al., 2021).

The main difference between jets and flares or eruptions is the size of the reconnection site. In the case of jets, the reconnection region is very small and the way how reconnection occurs is thus difficult to observe. Currently, it is impossible to resolve magnetic configurations at the reconnection site in the environment of jets. It is only by MHD simulations that we may assume the reconnection mechanism.

We show the importance of the role of photospheric motions and some attempts have been made to quantify the electric currents and related directly to recurrent jets (Guo et al., 2013). During emerging magnetic flux regions or filaments, the role of stress and accumulation of electric currents is important (Joshi et al., 2020b). However, many questions are still open, the transfer of twist, the role of the convection in the light bridge jets, the importance of the braiding of magnetic field lines to answer to coronal heating, the role of network jets in the corona as sources of solar wind. Solar Orbiter and Parker Solar Probe already brought some answers with their discoveries of campfires (Berghmans et al., 2021) and switchbacks of magnetic field (Bale et al., 2019; Ruffolo et al., 2020).

6. Acknowledgments

IRIS is a NASA small explorer mission developed and operated by LMSAL with mission operations executed at NASA Ames Research center and major contributions to downlink communications funded by the Norwegian Space Center (NSC, Norway) through an ESA PRODEX contract. We thank the SDO/AIA, SDO/HMI, and IRIS science teams for granting free access to the data. We thank the reviewers for their valuable suggestions which were quite important for us to improve the paper. RJ thanks to CEFIPRA for the Indo-French Raman Charpak fellowship. RJ and RC acknowledge the support from Bulgarian Science Fund under Indo-Bulgarian bilateral project, DST/INT/BLR/P-11/2019. This paper was presented at the COSPAR 2020 General Assembly session E2.2 in February 2021.

References

Antolin, P., Pagano, P., Testa, P., Petralia, A., & Reale, F. (2021). Reconnection nanojets in the solar corona. *Nature Astronomy*, *5*, 54–62. doi:10.1038/s41550-020-1199-8.

Archontis, V., & Hood, A. W. (2009). Formation of Ellerman bombs due to 3D flux emergence. *Astron. Astrophys.*, *508*(3), 1469–1483. doi:10.1051/0004-6361/200912455.

Asai, A., Ishii, T. T., & Kurokawa, H. (2001). Plasma Ejections from a Light Bridge in a Sunspot Umbra. *Astrophys. J. Lett.*, *555*, L65–L68. doi:10.1086/321738. arXiv:astro-ph/0111021.

Aulanier, G., & Dudík, J. (2019). Drifting of the line-tied footpoints of CME flux-ropes. *Astron. Astrophys.*, *621*, A72. doi:10.1051/0004-6361/201834221. arXiv:1811.04253.

Aulanier, G., Janvier, M., & Schmieder, B. (2012). The standard flare model in three dimensions. I. Strong-to-weak shear transition in post-flare loops. *Astron. Astrophys.*, *543*, A110. doi:10.1051/0004-6361/201219311.

Bale, S. D., Badman, S. T., Bonnell, J. W., Bowen, T. A., Burgess, D., Case, A. W., Cattell, C. A., Chandran, B. D. G., Chaston, C. C., Chen, C. H. K., Drake, J. F., de Wit, T. D., Eastwood, J. P., Ergun, R. E., Farrell, W. M., Fong, C., Goetz, K., Goldstein, M., Goodrich, K. A., Harvey, P. R., Horbury, T. S., Howes, G. G., Kasper, J. C., Kellogg, P. J., Klimchuk, J. A., Korreck, K. E., Krasnoselskikh, V. V., Krucker, S., Laker, R., Larson, D. E., MacDowall, R. J., Maksimovic, M., Malaspina, D. M., Martinez-Oliveros, J., McComas, D. J., Meyer-Vernet, N., Moncuquet, M., Mozer, F. S., Phan, T. D., Pulupa, M., Raouafi, N. E., Salem, C., Stansby, D., Stevens, M., Szabo, A., Velli, M., Woolley, T., & Wygant, J. R. (2019). Highly structured slow solar wind emerging from an equatorial coronal hole. *Nature*, *576*(7786), 237–242. doi:10.1038/s41586-019-1818-7.

Berghmans, D., Auchère, F., Long, D. M., Soubrié, E., Zhukov, A. N., Mierla, M., Schühle, U., Antolin, P., Parenti, S., Harra, L., Podladchikova, O., Aznar Cuadrado, R., Buchlin, É., Dolla, L., Verbeeck, C., Gissot, S., Teriaca, L., Haberreiter, M., Katsiyannis, A. C., Rodriguez, L., Kraaikamp, E., Smith, P. J., Stegen, K., Rochus, P., Halain, J. P., Jacques, L., Thompson, W. T., & Inhester, B. (2021). Extreme UV quiet Sun brightenings observed by Solar Orbiter/EUI. *arXiv e-prints*, (p. arXiv:2104.03382). arXiv:2104.03382.

Bharti, L. (2015). Fine structure above a light bridge in the transition region and corona. *Mon. Not. Roy. Astron. Soc.*, *452*(1), L16–L20. doi:10.1093/mnrasl/slv071. arXiv:1505.02412.

Bharti, L., Rimmele, T., Jain, R., Jaaffrey, S. N. A., & Smartt, R. N. (2007). Detection of opposite polarities in a sunspot light bridge: evidence of low-altitude magnetic reconnection. *Mon. Not. Roy. Astron. Soc.*, *376*(3), 1291–1295. doi:10.1111/j.1365-2966.2007.11525.x. arXiv:astro-ph/0701674.

Bharti, L., Sobha, B., Quintero Noda, C., Joshi, C., & Pandya, U. (2020). Chromospheric plasma ejection above a pore. *Mon. Not. Roy. Astron. Soc.*, *493*(2), 3036–3044. doi:10.1093/mnras/staa434. arXiv:2002.04503.

Cai, Q., Shen, C., Ni, L., Reeves, K. K., Kang, K., & Lin, J. (2019). Multi-band Study of a Bidirectional Jet Occurred in the Upper Chromosphere. *Journal of Geophysical Research (Space Physics)*, *124*(12), 9824–9846. doi:10.1029/2019JA027017.

Chae, J., Qiu, J., Wang, H., & Goode, P. R. (1999). Extreme-Ultraviolet Jets and Hα Surges in Solar Microflares. *Astrophys. J. Lett.*, *513*, L75–L78. doi:10.1086/311910.

Chandra, R., Gupta, G. R., Mulay, S., & Tripathi, D. (2015). Sunspot waves and triggering of homologous active region jets. *Mon. Not. Roy. Astron. Soc.*, *446*, 3741–3748. doi:10.1093/mnras/stu2305. arXiv:1410.8315.

Chandra, R., Mandrini, C. H., Schmieder, B., Joshi, B., Cristiani, G. D., Cremades, H., Pariat, E., Nuevo, F. A., Srivastava, A. K., & Uddin, W. (2017). Blowout jets and impulsive eruptive flares in a bald-patch topology. *Astron. Astrophys.*, *598*, A41. doi:10.1051/0004-6361/201628984. arXiv:1610.01918.

Chen, H., Zhang, J., De Pontieu, B., Ma, S., Kliem, B., & Priest, E. (2020). Coronal Mini-jets in an Activated Solar Tornado-like Prominence. *Astrophys. J.*, *899*(1), 19. doi:10.3847/1538-4357/ab9cad. arXiv:2006.08252.

Chen, H., Zhang, J., Ma, S., Yan, X., & Xue, J. (2017). Solar Tornadoes Triggered by Interaction between Filaments and EUV Jets. *Astrophys. J. Lett.*, *841*(1), L13. doi:10.3847/2041-8213/aa71a2.

Cheung, M. C. M., De Pontieu, B., Tarbell, T. D., Fu, Y., Tian, H., Testa, P., Reeves, K. K., Martínez-Sykora, J., Boerner, P., Wülser, J. P., Lemen, J., Title, A. M., Hurlburt, N., Kleint, L., Kankelborg, C., Jaeggli, S., Golub, L., McKillop, S., Saar, S., Carlsson, M., & Hansteen, V. (2015). Homologous Helical Jets: Observations By IRIS, SDO, and Hinode and Magnetic Modeling With Data-Driven Simulations. *Astrophys. J.*, *801*, 83. doi:10.1088/0004-637X/801/2/83. arXiv:1501.01593.

Chitta, L. P., Peter, H., & Li, L. (2019). Hot prominence spicules launched from turbulent cool solar prominences. *Astron. Astrophys.*, *627*, L5. doi:10.1051/0004-6361/201936027. arXiv:1906.09125.

Curdt, W., & Tian, H. (2011). Spectroscopic evidence for helicity in explosive events. *Astron. Astrophys.*, *532*, L9. doi:10.1051/0004-6361/201117116. arXiv:1107.1969.

Curdt, W., Tian, H., & Kamio, S. (2012). Explosive Events: Swirling Transition Region Jets. *Solar Phys.*, *280*, 417–424. doi:10.1007/s11207-012-9940-9. arXiv:1201.3199.

De Pontieu, B., Polito, V., Hansteen, V., Testa, P., Reeves, K. K., Antolin, P., Nóbrega-Siverio, D. E., Kowalski, A. F., Martinez-Sykora, J., Carlsson, M., McIntosh, S. W., Liu, W., Daw, A., & Kankelborg, C. C. (2021). A New View of the Solar Interface Region from the Interface Region Imaging Spectrograph (IRIS). *Solar Phys.*, *296*(5), 84. doi:10.1007/s11207-021-01826-0. arXiv:2103.16109.

De Pontieu, B., Title, A. M., Lemen, J. R., Kushner, G. D., Akin, D. J., Allard, B., Berger, T., Boerner, P., Cheung, M., Chou, C., Drake, J. F., Duncan, D. W., Freeland, S., Heyman, G. F., Hoffman, C., Hurlburt, N. E., Lindgren, R. W., Mathur, D., Rehse, R., Sabolish, D., Seguin, R., Schrijver, C. J., Tarbell, T. D., Wülser, J.-P., Wolfson, C. J., Yanari, C., Mudge, J., Nguyen-Phuc, N., Timmons, R., van Bezooijen, R., Weingrod, I., Brookner, R., Butcher, G., Dougherty, B., Eder, J., Knagenhjelm, V., Larsen, S., Mansir, D., Phan, L., Boyle, P., Cheimets, P. N., DeLuca, E. E., Golub, L., Gates, R., Hertz, E., McKillop, S., Park, S., Perry, T., Podgorski, W. A., Reeves, K., Saar, S., Testa, P., Tian, H., Weber, M., Dunn, C., Eccles, S., Jaeggli, S. A., Kankelborg, C. C., Mashburn, K., Pust, N., Springer, L., Carvalho, R., Kleint, L., Marmie, J., Mazmanian, E., Pereira, T. M. D., Sawyer, S., Strong, J., Worden, S. P., Carlsson, M., Hansteen, V. H., Leenaarts, J., Wiesmann, M., Aloise, J., Chu, K.-C., Bush, R. I., Scherrer, P. H., Brekke, P., Martinez-Sykora, J., Lites, B. W., McIntosh, S. W., Uitenbroek, H., Okamoto, T. J., Gummin, M. A., Auker, G., Jerram, P., Pool, P., & Waltham, N. (2014). The Interface Region Imaging Spectrograph (IRIS). *Solar Phys.*, *289*, 2733–2779. doi:10.1007/s11207-014-0485-y. arXiv:1401.2491.

Demoulin, P., & Priest, E. R. (1997). The Importance of Photospheric Intense Flux Tubes for Coronal Heating. *Solar Phys.*, *175*(1), 123–155. doi:10.1023/A:1004986503291.

Fang, F., Fan, Y., & McIntosh, S. W. (2014). Rotating Solar Jets in Simulations of Flux Emergence with Thermal Conduction. *Astrophys. J. Lett.*, *789*(1), L19. doi:10.1088/2041-8205/789/1/L19. arXiv:1406.2220.

Grubecka, M., Schmieder, B., Berlicki, A., Heinzel, P., Dalmasse, K., & Mein, P. (2016). Height formation of bright points observed by IRIS in Mg II line wings during flux emergence. *Astron. Astrophys.*, *593*, A32. doi:10.1051/0004-6361/201527358.

Guo, Y., Démoulin, P., Schmieder, B., Ding, M. D., Vargas Domínguez, S., & Liu, Y. (2013). Recurrent coronal jets induced by repetitively accumulated electric currents. *Astron. Astrophys.*, *555*, A19. doi:10.1051/0004-6361/201321229. arXiv:1305.0902.

Hansteen, V., Ortiz, A., Archontis, V., Carlsson, M., Pereira, T. M. D., & Bjørgen, J. P. (2019). Ellerman bombs and UV bursts: transient events in chromospheric current sheets. *Astron. Astrophys.*, *626*, A33. doi:10.1051/0004-6361/201935376. arXiv:1904.11524.

Harrison, R. A., Sawyer, E. C., Carter, M. K., Cruise, A. M., Cutler, R. M., Fludra, A., Hayes, R. W., Kent, B. J., Lang, J., Parker, D. J., Payne, J., Pike, C. D., Peskett, S. C., Richards, A. G., Gulhane, J. L., Norman, K., Breeveld, A. A., Breeveld, E. R., Al Janabi, K. F., McCalden, A. J., Parkinson, J. H., Self, D. G., Thomas, P. D., Poland, A. I., Thomas, R. J., Thompson, W. T., Kjeldseth-Moe, O., Brekke, P., Karud, J., Maltby, P., Aschenbach, B., Bräuninger, H., Kühne, M., Hollandt, J., Siegmund, O. H. W., Huber, M. C. E., Gabriel, A. H., Mason, H. E., & Bromage, B. J. I. (1995). The Coronal Diagnostic Spectrometer for the Solar and Heliospheric Observatory. *Solar Phys.*, *162*(1-2), 233–290. doi:10.1007/BF00733431.

Heinzel, P., & Kleint, L. (2014). Hydrogen Balmer Continuum in Solar Flares Detected by the Interface Region Imaging Spectrograph (IRIS). *Astrophys. J. Lett.*, *794*(2), L23. doi:10.1088/2041-8205/794/2/L23. arXiv:1409.5680.

Huang, Z., Xia, L., Nelson, C. J., Liu, J., Wiegelmann, T., Tian, H., Klimchuk, J. A., Chen, Y., & Li, B. (2018). Magnetic Braids in Eruptions of a Spiral Structure in the Solar Atmosphere. *Astrophys. J.*, *854*(2), 80. doi:10.3847/1538-4357/aaa9ba. arXiv:1801.05967.

Janvier, M., Aulanier, G., Pariat, E., & Démoulin, P. (2013). The standard flare model in three dimensions. III. Slip-running reconnection properties. *Astron. Astrophys.*, *555*, A77. doi:10.1051/0004-6361/201321164. arXiv:1305.4053.

Jiang, Y. C., Chen, H. D., Li, K. J., Shen, Y. D., & Yang, L. H. (2007). The Hα surges and EUV jets from magnetic flux emergences and cancellations. *Astron. Astrophys.*, *469*, 331–337. doi:10.1051/0004-6361:20053954.

Joshi, R., Chandra, R., Schmieder, B., Moreno-Insertis, F., Aulanier, G., Nóbrega-Siverio, D., & Devi, P. (2020a). Case study of multi-temperature coronal jets for emerging flux MHD models. *Astron. Astrophys.*, *639*, A22. doi:10.1051/0004-6361/202037806. arXiv:2005.06064.

Joshi, R., Schmieder, B., Aulanier, G., Bommier, V., & Chandra, R. (2020b). The role of small-scale surface motions in the transfer of twist to a solar jet from a remote stable flux rope. *Astron. Astrophys.*, *642*, A169. doi:10.

1051/0004-6361/202038562. arXiv:2008.06887.
Joshi, R., Schmieder, B., Chandra, R., Aulanier, G., Zuccarello, F. P., & Uddin, W. (2017). Slippage of Jets Explained by the Magnetic Topology of NOAA Active Region 12035. *Solar Phys.*, *292*, 152. doi:10.1007/s11207-017-1176-2. arXiv:1709.02791.
Joshi, R., Schmieder, B., Heinzel, P., Tomin, J., Chandra, R., & Vilmer, N. (2021b). Balmer continuum enhancement detected in a mini flare observed with IRIS. *Astron. Astrophys.*, *654*, A31. doi:10.1051/0004-6361/202141172. arXiv:2107.11651.
Joshi, R., Schmieder, B., Tei, A., Aulanier, G., Lörinčík, J., Chandra, R., & Heinzel, P. (2021a). Multi-thermal atmosphere of a mini-solar flare during magnetic reconnection observed with IRIS. *Astron. Astrophys.*, *645*, A80. doi:10.1051/0004-6361/202039229. arXiv:2010.15401.
Judge, P. G. (2015). UV Spectra, Bombs, and the Solar Atmosphere. *Astrophys. J.*, *808*(2), 116. doi:10.1088/0004-637X/808/2/116. arXiv:1506.08336.
Kamio, S., Hara, H., Watanabe, T., Matsuzaki, K., Shibata, K., Culhane, L., & Warren, H. P. (2007). Velocity Structure of Jets in a Coronal Hole. *Pub. Astron. Soc. Japan*, *59*, S757. doi:10.1093/pasj/59.sp3.S757. arXiv:0711.2848.
Kayshap, P., & Dwivedi, B. N. (2017). Diagnostics of Coronal Bright Points using IRIS, AIA, and HMI Observations. *Solar Phys.*, *292*(8), 108. doi:10.1007/s11207-017-1132-1.
Kayshap, P., Singh Payal, R., Tripathi, S. C., & Padhy, H. (2021). Diagnostics of homologous solar-surge plasma as observed by IRIS and SDO. *Mon. Not. Roy. Astron. Soc.*, *505*(4), 5311–5326. doi:10.1093/mnras/stab1663. arXiv:2106.06222.
Kim, Y.-H., Kim, K.-S., & Jang, M. (2001). High-Speed x-ray Jets Associated with the 18 June 1999 Limb Flares. *Solar Phys.*, *203*(2), 371–379. doi:10.1023/A:1013324126229.
Kleint, L., Heinzel, P., Judge, P., & Krucker, S. (2016). Continuum Enhancements in the Ultraviolet, the Visible and the Infrared during the X1 Flare on 2014 March 29. *Astrophys. J.*, *816*(2), 88. doi:10.3847/0004-637X/816/2/88. arXiv:1511.04161.
Kleint, L., Heinzel, P., & Krucker, S. (2017). On the Origin of the Flare Emission in IRIS' SJI 2832 Filter:Balmer Continuum or Spectral Lines? *Astrophys. J.*, *837*(2), 160. doi:10.3847/1538-4357/aa62fe. arXiv:1702.07167.
Lemen, J. R., Title, A. M., Akin, D. J., Boerner, P. F., Chou, C., Drake, J. F., Duncan, D. W., Edwards, C. G., Friedlaender, F. M., Heyman, G. F., Hurlburt, N. E., Katz, N. L., Kushner, G. D., Levay, M., Lindgren, R. W., Mathur, D. P., McFeaters, E. L., Mitchell, S., Rehse, R. A., Schrijver, C. J., Springer, L. A., Stern, R. A., Tarbell, T. D., Wuelser, J.-P., Wolfson, C. J., Yanari, C., Bookbinder, J. A., Cheimets, P. N., Caldwell, D., Deluca, E. E., Gates, R., Golub, L., Park, S., Podgorski, W. A., Bush, R. I., Scherrer, P. H., Gummin, M. A., Smith, P., Auker, G., Jerram, P., Pool, P., Soufli, R., Windt, D. L., Beardsley, S., Clapp, M., Lang, J., & Waltham, N. (2012). The Atmospheric Imaging Assembly (AIA) on the Solar Dynamics Observatory (SDO). *Solar Phys.*, *275*, 17–40. doi:10.1007/s11207-011-9776-8.
Meegan, C., Lichti, G., Bhat, P. N., Bissaldi, E., Briggs, M. S., Connaughton, V., Diehl, R., Fishman, G., Greiner, J., Hoover, A. S., van der Horst, A. J., von Kienlin, A., Kippen, R. M., Kouveliotou, C., McBreen, S., Paciesas, W. S., Preece, R., Steinle, H., Wallace, M. S., Wilson, R. B., & Wilson-Hodge, C. (2009). The Fermi Gamma-ray Burst Monitor. *Astrophys. J.*, *702*(1), 791–804. doi:10.1088/0004-637X/702/1/791. arXiv:0908.0450.
Moreno-Insertis, F., & Galsgaard, K. (2013). Plasma Jets and Eruptions in Solar Coronal Holes: A Three-dimensional Flux Emergence Experiment. *Astrophys. J.*, *771*, 20. doi:10.1088/0004-637X/771/1/20. arXiv:1305.2201.
Moreno-Insertis, F., Galsgaard, K., & Ugarte-Urra, I. (2008). Jets in Coronal Holes: Hinode Observations and Three-dimensional Computer Modeling. *Astrophys. J. Lett.*, *673*, L211–L214. doi:10.1086/527560. arXiv:0712.1059.
Mulay, S. (2018). *EUV Spectroscopy of Solar Active Region Jets*. Ph.D. thesis Department of Applied Mathematics and Theoretical Physics, University of Cambridge, UK. doi:https://doi.org/10.17863/CAM.25040.
Mulay, S. M., Del Zanna, G., & Mason, H. (2017a). Cool and hot emission in a recurring active region jet. *Astron. Astrophys.*, *606*, A4. doi:10.1051/0004-6361/201730429.
Mulay, S. M., Del Zanna, G., & Mason, H. (2017b). Temperature and density structure of a recurring active region jet. *Astron. Astrophys.*, *598*, A11. doi:10.1051/0004-6361/201628796. arXiv:1609.08472.
Mulay, S. M., Tripathi, D., Del Zanna, G., & Mason, H. (2016). Multiwavelength study of 20 jets that emanate from the periphery of active regions. *Astron. Astrophys.*, *589*, A79. doi:10.1051/0004-6361/201527473. arXiv:1602.00151.
Ni, L., Chen, Y., Peter, H., Tian, H., & Lin, J. (2021). A magnetic reconnection model for hot explosions in the cool atmosphere of the Sun. *Astron. Astrophys.*, *646*, A88. doi:10.1051/0004-6361/202039239. arXiv:2011.07692.
Ni, L., Lin, J., Roussev, I. I., & Schmieder, B. (2016). Heating Mechanisms in the Low Solar Atmosphere through Magnetic Reconnection in Current Sheets. *Astrophys. J.*, *832*(2), 195. doi:10.3847/0004-637X/832/2/195. arXiv:1611.01746.
Nóbrega Siverio, D., Guglielmino, S. L., & Sainz Dalda, A. (2021). Solar surges related to UV bursts: Characterization through k-means, inversions and density diagnostics. *arXiv e-prints*, (p. arXiv:2108.13960). arXiv:2108.13960.
Nóbrega-Siverio, D., Martínez-Sykora, J., Moreno-Insertis, F., & Rouppe van der Voort, L. (2017). Surges and Si IV Bursts in the Solar Atmosphere: Understanding IRIS and SST Observations through RMHD Experiments. *Astrophys. J.*, *850*, 153. doi:10.3847/1538-4357/aa956c. arXiv:1710.08928.
Pariat, E., Antiochos, S. K., & DeVore, C. R. (2009). A Model for Solar Polar Jets. *Astrophys. J.*, *691*, 61–74. doi:10.1088/0004-637X/691/1/61.
Pariat, E., Dalmasse, K., DeVore, C. R., Antiochos, S. K., & Karpen, J. T. (2016). A model for straight and helical solar jets. II. Parametric study of the plasma beta. *Astron. Astrophys.*, *596*, A36. doi:10.1051/0004-6361/201629109. arXiv:1609.08825.
Parker, E. N. (1988). Nanoflares and the Solar X-Ray Corona. *Astrophys. J.*, *330*, 474. doi:10.1086/166485.
Pesnell, W. D., Thompson, B. J., & Chamberlin, P. C. (2012). The Solar Dynamics Observatory (SDO). *Solar Phys.*, *275*, 3–15. doi:10.1007/s11207-011-9841-3.
Peter, H., Tian, H., Curdt, W., Schmit, D., Innes, D., De Pontieu, B., Lemen, J., Title, A., Boerner, P., Hurlburt, N., Tarbell, T. D., Wuelser, J. P., Martínez-Sykora, J., Kleint, L., Golub, L., McKillop, S., Reeves, K. K., Saar, S., Testa, P., Kankelborg, C., Jaeggli, S., Carlsson, M., & Hansteen, V. (2014). Hot explosions in the cool atmosphere of the Sun. *Science*, *346*, 1255726. doi:10.1126/science.1255726. arXiv:1410.5842.
Pike, C. D., & Mason, H. E. (1998). Rotating Transition Region Features Observed with the SOHO Coronal Diagnostic Spectrometer. *Solar Phys.*, *182*(2), 333–348. doi:10.1023/A:1005065704108.
Polito, V., Del Zanna, G., Dudík, J., Mason, H. E., Giunta, A., & Reeves, K. K. (2016). Density diagnostics derived from the O iv and S iv intercombination lines observed by IRIS. *Astron. Astrophys.*, *594*, A64. doi:10.1051/0004-6361/201628965. arXiv:1607.05072.
Priest, E. R., Chitta, L. P., & Syntelis, P. (2018). A Cancellation Nanoflare Model for Solar Chromospheric and Coronal Heating. *Astrophys. J. Lett.*, *862*(2), L24. doi:10.3847/2041-8213/aad4fc. arXiv:1807.08161.
Raouafi, N. E., Patsourakos, S., Pariat, E., Young, P. R., Sterling, A. C., Savcheva, A., Shimojo, M., Moreno-Insertis, F., DeVore, C. R., Archontis, V., Török, T., Mason, H., Curdt, W., Meyer, K., Dalmasse, K., & Matsui, Y. (2016). Solar Coronal Jets: Observations, Theory, and Modeling. *Space Sci. Rev.*, *201*, 1–53. doi:10.1007/s11214-016-0260-5. arXiv:1607.02108.
Robustini, C., Leenaarts, J., de la Cruz Rodriguez, J., & Rouppe van der Voort, L. (2016). Fan-shaped jets above the light bridge of a sunspot driven by reconnection. *Astron. Astrophys.*, *590*, A57. doi:10.1051/0004-6361/201528022. arXiv:1508.07927.
Rompolt, B. (1975). Spectral Features to be Expected from Rotational and Expansional Motions in Fine Solar Structures. *Solar Phys.*, *41*(2), 329–348. doi:10.1007/BF00154070.
Roy, J. R. (1973). The Magnetic Properties of Solar Surges. *Solar Phys.*, *28*, 95–114. doi:10.1007/BF00152915.
Ruan, G., Schmieder, B., Masson, S., Mein, P., Mein, N., Aulanier, G., & Chen, Y. (2019). Bidirectional Reconnection Outflows in an Active Region. *Astrophys. J.*, *883*(1), 52. doi:10.3847/1538-4357/ab3657.
Ruffolo, D., Matthaeus, W. H., Chhiber, R., Usmanov, A. V., Yang, Y., Bandyopadhyay, R., Parashar, T. N., Goldstein, M. L., DeForest, C. E., Wan, M., Chasapis, A., Maruca, B. A., Velli, M., & Kasper, J. C. (2020). Shear-driven

Transition to Isotropically Turbulent Solar Wind Outside the Alfvén Critical Zone. *Astrophys. J.*, *902*(2), 94. doi:10.3847/1538-4357/abb594. arXiv:2009.06537.

Schmieder, B., Guo, Y., Moreno-Insertis, F., Aulanier, G., Yelles Chaouche, L., Nishizuka, N., Harra, L. K., Thalmann, J. K., Vargas Dominguez, S., & Liu, Y. (2013). Twisting solar coronal jet launched at the boundary of an active region. *Astron. Astrophys.*, *559*, A1. doi:10.1051/0004-6361/201322181. arXiv:1309.6514.

Schmieder, B., Mein, P., Simnett, G. M., & Tandberg-Hanssen, E. (1988). An example of the association of X-ray and UV emission with H-alpha surges. *Astron. Astrophys.*, *201*(2), 327–338.

Schmieder, B., Mein, P., Vial, J.-C., & Tandberg-Hanssen, E. (1983). Dynamics of a surge observed in the C IV and H alpha lines. *Astron. Astrophys.*, *127*, 337–344.

Schmieder, B., Shibata, K., van Driel-Gesztelyi, L., & Freeland, S. (1995). H alpha surges and associated soft X-ray loops. *Solar Phys.*, *156*, 245–264. doi:10.1007/BF00670226.

Shen, Y. (2021). Observation and modelling of solar jets. *Proceedings of the Royal Society of London Series A*, *477*(2246), 217. doi:10.1098/rspa.2020.0217. arXiv:2101.04846.

Shibata, K., Nozawa, S., & Matsumoto, R. (1992). Magnetic reconnection associated with emerging magnetic flux. *PASJ*, *44*, 265–272.

Shimizu, T. (2011). Long-term Evolution of Magnetic and Dynamical Properties in A Sunspot Light Bridge. *Astrophys. J.*, *738*(1), 83. doi:10.1088/0004-637X/738/1/83.

Shimizu, T., Katsukawa, Y., Kubo, M., Lites, B. W., Ichimoto, K., Suematsu, Y., Tsuneta, S., Nagata, S., Shine, R. A., & Tarbell, T. D. (2009). Hinode Observation of the Magnetic Fields in a Sunspot Light Bridge Accompanied by Long-Lasting Chromospheric Plasma Ejections. *Astrophys. J. Lett.*, *696*(1), L66–L69. doi:10.1088/0004-637X/696/1/L66.

Sterling, A. C., Moore, R. L., Falconer, D. A., Panesar, N. K., Akiyama, S., Yashiro, S., & Gopalswamy, N. (2016). Minifilament Eruptions that Drive Coronal Jets in a Solar Active Region. *Astrophys. J.*, *821*, 100. doi:10.3847/0004-637X/821/2/100.

Toriumi, S., Katsukawa, Y., & Cheung, M. C. M. (2015). Light Bridge in a Developing Active Region. I. Observation of Light Bridge and its Dynamic Activity Phenomena. *Astrophys. J.*, *811*(2), 137. doi:10.1088/0004-637X/811/2/137. arXiv:1509.00183.

Török, T., Aulanier, G., Schmieder, B., Reeves, K. K., & Golub, L. (2009). Fan-Spine Topology Formation Through Two-Step Reconnection Driven by Twisted Flux Emergence. *Astrophys. J.*, *704*, 485–495. doi:10.1088/0004-637X/704/1/485. arXiv:0909.2235.

Uddin, W., Schmieder, B., Chandra, R., Srivastava, A. K., Kumar, P., & Bisht, S. (2012). Observations of Multiple Surges Associated with Magnetic Activities in AR 10484 on 2003 October 25. *Astrophys. J.*, *752*(1), 70. doi:10.1088/0004-637X/752/1/70. arXiv:1204.2053.

Wilhelm, K., Curdt, W., Marsch, E., Schühle, U., Lemaire, P., Gabriel, A., Vial, J. C., Grewing, M., Huber, M. C. E., Jordan, S. D., Poland, A. I., Thomas, R. J., Kühne, M., Timothy, J. G., Hassler, D. M., & Siegmund, O. H. W. (1995). SUMER - Solar Ultraviolet Measurements of Emitted Radiation. *Solar Phys.*, *162*(1-2), 189–231. doi:10.1007/BF00733430.

Wyper, P. F., DeVore, C. R., & Antiochos, S. K. (2019). Numerical simulation of helical jets at active region peripheries. *Mon. Not. Roy. Astron. Soc.*, *490*(3), 3679–3690. doi:10.1093/mnras/stz2674. arXiv:1909.09423.

Yang, S., Zhang, Q., Xu, Z., Zhang, J., Zhong, Z., & Guo, Y. (2020). Imaging and spectral study on the null point of a fan-spine structure during a solar flare. *arXiv e-prints*, (p. arXiv:2005.09613). arXiv:2005.09613.